Available online at www.sciencedirect.com
SCIENCE DIRECT®
Journal of Solid State Chemistry 179 (2006) 355–361
JOURNAL OF SOLID STATE CHEMISTRY
www.elsevier.com/locate/jssc

Neutron diffraction and electrochemical studies on $LiIrSn_4$

Puravankara Sreeraj[a], Hans-Dieter Wiemhöfer[a], Rolf-Dieter Hoffmann[a], Rolf Skowronek[b,c], Armin Kirfel[c], Rainer Pöttgen[a,*]

[a]*Institut für Anorganische und Analytische Chemie, NRW Graduate School of Chemistry and Sonderforschungsbereich 458, Universität Münster, Corrensstrasse 36, D-48149 Münster, Germany*
[b]*Forschungszentrum Jülich, Institut für Festkörperforschung, D-52425 Jülich, Germany*
[c]*Mineralogisch-Petrologisches Institut, Universität Bonn, Poppelsdorfer Schloß; D-53115 Bonn, Germany*

Received 24 August 2005; received in revised form 12 October 2005; accepted 20 October 2005
Available online 22 November 2005

Abstract

Large quantities of single phase, polycrystalline $LiIrSn_4$ have been synthesised from the elements by melting in sealed tantalum tubes and subsequent annealing. $LiIrSn_4$ crystallises with an ordered version of the $PdGa_5$ structure: $I4/mcm$, $a = 655.62(8)$, $c = 1128.6(2)$ pm. The lithium atoms were clearly localised from a neutron powder diffraction study: $R_P = 0.147$ and $R_F = 0.058$. Time-dependent electrochemical polarisation techniques, i.e. coulometric titration, chronopotentiometry, chronoamperometry and cyclic voltammetry were used to study the kinetics of lithium ion diffusion in this stannide. The range of homogeneity ($Li_{1+\Delta\delta}IrSn_4$, $-0.091 \leqslant \delta \leqslant +0.012$) without any structural change in the host structure and the chemical diffusion coefficient ($\sim 10^{-7}$–10^{-9} cm^2/s) point out that $LiIrSn_4$ is a first example of a large class of intermetallic compounds with lithium and electron mobility. Optimised materials from these ternary lithium alloys may be potential electrode material for rechargeable lithium batteries.

Keywords: Intermetallic compound; Electrochemistry; Ionic conductivity

1. Introduction

During the last decade, there has been a strongly increased interest in the development of materials for rechargeable cells, in particular for lithium batteries. The research concerned the increase in energy density as well as the improved long-term stability and kinetics of electrodes and electrolytes.

Commercial lithium ion batteries currently employ non-aqueous liquid and polymeric electrolytes, carbon anodes and cathodes made for instance of compounds such as layered lithium cobalt oxide. Novel useful materials for both cathodes and anodes have been reviewed by many authors. A recent report is given by Besenhard [1]. There are, however, limitations among the current electrode materials. For instance, only 50% of the theoretical capacity of lithium cobalt oxide can be used and cobalt is relatively expensive and toxic. Moreover, carbon anodes exhibit large irreversible capacities. Accordingly, investigations on potential novel electrode materials are desirable.

Lithium intermetallic compounds, either binary or ternary, have found renewed interest for the use as negative electrodes for lithium batteries. Extensive research has been done particularly on binary alloys [2–6] in order to replace the existing carbon-based anodes. Only a few reports have come through regarding ternary lithium intermetallic alloys [7,8] Among the intermetallics, tin alloys have obtained maximum attention due to the large reversible charge–discharge capacities which can be obtained for the highly dispersed material [9]. But in almost all the cases the Li-insertion in binary alloys is accompanied by large volume expansion, in some cases as large as 358% [5,10].

So the focus then turned to ternary intermetallic compounds which are not expected to develop these large critical volume expansions. The intermetallic material Li–In–Sb has been investigated for use as positive electrode

*Corresponding author. Fax: +49 251 83 36002.
E-mail addresses: r.skowronek@fz-juelich.de (R. Skowronek), kirfel@uni-bonn.de (A. Kirfel), pottgen@uni-muenster.de (R. Pöttgen).

0022-4596/$ - see front matter © 2005 Elsevier Inc. All rights reserved.
doi:10.1016/j.jssc.2005.10.026

material [8]. With this in mind, we started a systematic investigation of lithium-transition metal-stannides with respect to phase analyses, crystal chemistry and lithium mobility [11–16]. In this context, the new stannides $LiTSn_4$ (T = Ru, Rh, Ir) [14,15] have been synthesised and characterised by X-ray diffraction and temperature dependent ^{119}Sn Mössbauer and solid-state NMR spectroscopy. The structures of the $LiTSn_4$ stannides (Fig. 2) are characterised through [TSn_4] layers that are separated by the lithium atoms. The reason for choosing the iridium compound was its higher tendency to form ions compared with other noble metals [11,15]. Our first results gave hints that intermetallics like $LiIrSn_4$ may be candidates for electrode materials in lithium batteries. The presence of the noble metal definitely increases the electrode potential much above that of elemental lithium. Consequently, these materials may be seen as cathode materials in lithium ion batteries. It is not clear whether $LiIrSn_4$ could also be an anode material in combination with the 5 V cathode material reported in the literature [17].

To summarise, our investigations on ternary lithium alloys were aimed, looking for safe and stable electrode materials with potentials above that of metallic lithium, showing a moderate volume expansion and showing sufficiently good lithium ion diffusion. Accordingly, thermodynamic and kinetic properties play a role. First of all, the interest lies on the rate at which a mobile species can be added or deleted from the host structure or both [5,18–20]. If the surface exchange of lithium at the interface to an electrolyte is fast, the chemical diffusion coefficient of lithium D_{Li} is the most important kinetic parameter. Direct measurement of this parameter is possible from time-dependent electrochemical polarisation studies [6,18,19]. This contribution reports on the chemical diffusion kinetics of $LiIrSn_4$.

In parallel a bulk sample of $LiIrSn_4$ was studied by neutron diffraction. Owing to the weak scattering power of lithium using X-ray diffraction, the employment of neutron data should greatly enhance the determination of the lithium content of $LiIrSn_4$. The ratios of the scattering lengths of lithium (−1.90 fm), tin (5.68 fm) and iridium (10.6 fm) are more favorable for the refinement of lithium atoms and their occupancy parameter.

2. Theoretical considerations

The chemical diffusion coefficient as a function of lithium activity can be obtained using galvanostatic or potentiostatic polarisation experiments. Coulometric titration can be used, on the other hand, with the sample as an electrode in a galvanic cell and with a lithium ion containing electrolyte to intercalate and deintercalate lithium in binary and ternary alloys with high stoichiometric precision [8,21]. The combination of transient diffusion measurements and measurements of the equilibrium cell voltage as a function of composition is now a common electrochemical technique often termed as galvanostatic intermittent titration technique (GITT). This method which we apply here has been reviewed by Wen et al. [2] and Weppner et al. [19].

The working cell (PC = propylene carbonate) is

$$Li|LiCF_3SO_3 \text{ in PC(1M)}|Li_xIrSn_4$$

with metallic lithium as both the reference and the counter electrode. The electrolyte is a pure lithium ion conductor and the standard cell reaction consists of the transfer of 1 mol of lithium atoms from the lithium anode to the Li_xIrSn_4 cathode. Lithium is supposed to be the only mobile component in the cathode. The cell voltage E_{cell} depends on the composition x of the ternary alloy and is given by the difference of the chemical potentials of lithium of the two electrodes according to (with F = Faraday's constant)

$$E_{cell}\,F = -[\mu_{Li}(x) - \mu^{\circ}_{Li}]. \quad (1)$$

By coulometric titration the lithium content in the sample can be varied with stoichiometric precision. For this, one passes a series of constant current pulses I through the cell, each for a time interval τ and each pulse corresponding to the charge $I\tau$. The single pulses are separated by an intermediate time interval Δt that has to be long enough for the cell voltage to become nearly constant after switching-off the preceding current pulse. One monitors the transient behaviour of the voltage with time. The starting value of the lithium stoichiometry of our samples is virtually $LiIrSn_4$ that is x in the formula Li_xIrSn_4 is approximately $x = 1.00$. From the charge transported during a current pulse, the change $\Delta\delta$ of the lithium stoichiometry is calculated. Considering the polycrystalline ternary alloy $Li_{1+\Delta\delta}IrSn_4$ as a quasi-binary compound $Li_{1+\Delta\delta}B$, one can write

$$\Delta\delta = I\tau M_B/m_B F, \quad (2)$$

where M_B, m_B are the molecular weight of the host structure (= $IrSn_4$ denoted by B), and the mass m_B of B, respectively.

The final constant electrode potential at the time Δt after each current step plotted vs. the non-stoichiometry $\Delta\delta$ (referred to the starting composition) corresponds to the coulometric titration curve and thus gives the chemical potential of lithium in the compound as a function of composition.

For short times of current flow, $t \ll L^2/D_{Li}$, (L = thickness of the sample) and sufficiently small potential changes during a single galvanostatic current pulse, one can calculate the chemical diffusion coefficient D_{Li} according to

$$D_{Li} = (4/\pi\tau)(m_B V_M/M_B A)^2(\Delta E_s/\Delta E_t)^2. \quad (3)$$

V_M is the molar volume of the sample, A the total surface area of the sample in contact to the electrolyte. Here, the electrolyte was in contact with both sides of the electrode material. ΔE_s corresponds to the change of the steady-state voltage of the cell after each current pulse, and

ΔE_t denotes the total transient voltage change of the cell for an applied galvanostatic current I for the time τ (after compensation for the IR drop).

We also applied potentiostatic experiments to check the galvanostatic results for D_{Li}. In the potentiostatic mode, the time-dependent parameter is the electrical current. The potentiostatic method allows a more efficient control of the interface stoichiometry avoiding unwanted side reactions since voltages are held within the stability range of the single phase alloy. The solution of Fick's law predicts for the long-time approximation $t \gg L^2/D_{Li}$

$$I(t) = (2Q\, D_{Li}/L^2)\exp(-\pi^2 D_{Li} t/4L^2), \quad (4)$$

where $Q = I\tau$ denotes the amount of charge passed. Here, t is the time calculated from the beginning of each voltage step. For evaluation, we replaced L in the above equation by $L/2$ since the sample is in contact with the electrolyte on both sides. Therefore, the slope of $\ln[I(t)]$ vs. t should be a straight line and D_{Li} is obtained from the slope. For the details of the method and the equations, we refer to the publication by Weppner et al. [19].

3. Experimental

3.1. Synthesis and neutron diffraction

Polycrystalline samples of $LiIrSn_4$ were prepared by standard solid-state reactions in sealed tantalum ampoules as described previously [14,15]. Starting materials for the preparation of $LiIrSn_4$ were lithium rods (Merck, >99%), iridium powder (Degussa-Hüls, ca. 200 mesh, >99.9%) and a tin bar (Heraeus, >99.9%). The elements were mixed in the ideal atomic ratio and sealed in tantalum tubes under an argon pressure of about 600 mbar [22]. The tantalum tubes were sealed in evacuated silica ampoules, heated to 1170 K within 30 min, kept at that temperature for 5 h, cooled to 770 K in an hour, annealed at that temperature for 6 days and then finally quenched by radiative heat loss. About 5 g of $LiIrSn_4$ were synthesised for the neutron diffraction experiment. The purity of the different samples was checked through Guinier powder patterns using Cu$K\alpha_1$ radiation and α-quartz ($a = 491.30$, $c = 540.46$ pm) as an internal standard. The experimental patterns were compared with a calculated one [23], using the previously reported single crystal data [15].

Neutron diffraction was employed at room temperature using the SV-7 powder diffractometer with a radially oscillating collimator in front of the position-sensitive detector and a wavelength of 109.59 pm at the FRJ-2 reactor in Jülich. The sample was filled in a cylindrical vanadium container. Data were collected for 11 h and accumulated to a step width of 0.1° in 2θ. Full-pattern Rietveld refinements using FULLPROF [24] have been performed.

3.2. Electrochemistry

For the electrochemical investigation, the material was ground and uniaxially pressed into disk-shaped samples of thickness ~0.5–0.9 mm and diameter 6 mm. Initially, they were pressed uniaxially under a force of 20 kN for 20 min. For electrical contact a Pt wire of thickness 0.1 mm was embedded into the sample during pressing. By this we could avoid the use of graphite to provide good electrical contact during the measurements. Later on, these pellets were pressed under a force of 900 kN for 2 h.

The electrochemical measurements were carried out on samples that were prepared with 3% of polyvinylidene fluoride (PVDF) in order to provide mechanical stability. A standard three electrode cell was used for the measurements [19]. Pure Li metal in the form of rods served both as a reference and counter electrodes. As electrolyte $LiCF_3SO_3$ in PC (1 mol/L) was used. The cell was assembled and placed inside an argon-filled glove box. The H_2O content of the glove box was maintained below 20 ppm. All the measurements were carried out inside the glove box and results were checked for reproducibility. Neither crumbling of the pelletised polycrystalline sample nor loss of electrical contact was observed during the galvanostatic and potentiostatic measurements.

Coulometric titration was performed by applying intermittent galvanostatic current pulses (current density 0.25 A/cm^2). The cell voltage was observed both during and after the current pulses. After each current pulse, sufficient time (generally 2 h) was given for attaining equilibrium potential. Coulometric titration curves were evaluated from the amounts of charge transferred during the pulses and the equilibrium potentials after each current pulse between 3 and 1.6 V vs. Li reference.

In the potentiostatic experiments, a constant polarisation voltage was applied at least for 2 h, during steady state and transient measurements in order to apply the long-time approximations for evaluation. In addition, cyclic voltammetry was carried out in the voltage range 0 and 3 V at a scan rate of 1 mV/s.

Ohmic voltage drops were evaluated for both GITT and potentiostatic techniques and the usual IR correction was applied. Potentials, currents and charges were measured using a potentiostat (PAR, model 283.)

4. Results and discussion

4.1. Neutron diffraction and crystal chemistry

Fig. 1 presents the neutron diffraction pattern of $LiIrSn_4$ recorded at room temperature. The lattice parameters nicely match those derived from X-ray diffraction [15] ($a = 657.34(5)$, $c = 1130.4(1)$ pm): $\lambda = 109.59$ pm, $a = 655.62(8)$ and $c = 1128.6(2)$; space group $I4/mcm$; $R_P = 14.7$ and $R_F = 5.8$. Lithium occupies the site 4c (0, 0, 0), iridium and tin the sites 4a (0, 0, 1/4) and 16l (0.1575(5), 1/2−x, 0.3670(3)), respectively.

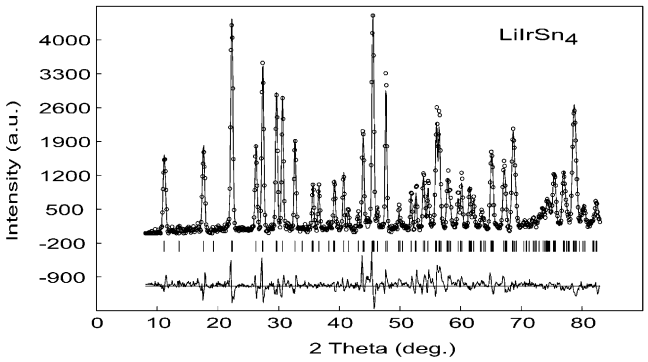

Fig. 1. Rietveld refinement plot for $LiIrSn_4$, in which the observed intensities are indicated with open circles and the calculated pattern with a line on top of the circles. The vertical lines indicate the Bragg positions. The difference I(obs)–I(calc) is drawn below the Bragg indicators.

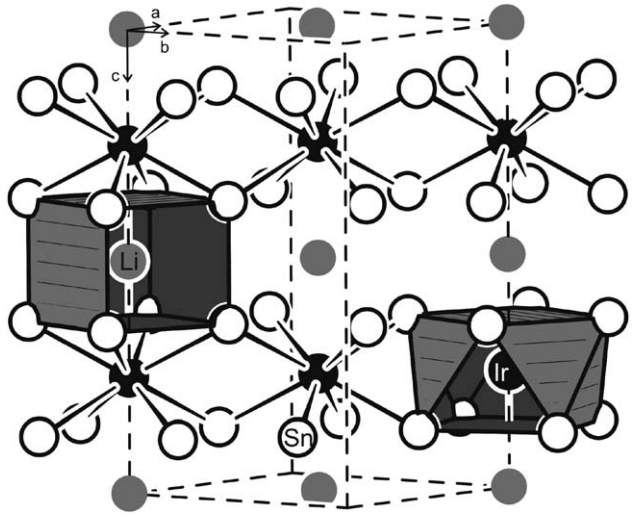

Fig. 2. Crystal structure of tetragonal $LiIrSn_4$, space group $I4/mcm$. Lithium, iridium, and tin atoms are drawn as grey, filled, and open circles, respectively. The two-dimensional $[IrSn_4]$ network, the square-prismatic lithium and the square antiprismatic iridium coordination are emphasised.

The positional parameters determined for $LiIrSn_4$ from the neutron powder diffraction data are in good agreement with the X-ray data ($x_{Sn} = 0.15814(5)$ and $z_{Sn} = 0.36556(6)$) [15]. Whereas the lithium occupancy could not be refined well with X-ray data, the neutron data allowed to refine the lithium site occupancy and also to obtain reasonable displacement parameters for lithium. The refined values were $B(Li) = 1.1(4)\text{Å}^2$, $B(Ir) = 0.58(8)\text{Å}^2$, $B(Sn) = 0.77(7)\text{Å}^2$. The lithium occupancy parameter of 100(8)% was refined in a separate series of least-squares cycles. Since the refinement revealed full occupancy within one standard uncertainty, the ideal occupancy was assumed in the final cycles.

The crystal structure of $LiIrSn_4$ is presented in Fig. 2. Since the crystal chemistry and chemical bonding has been discussed in detail in previous manuscripts, we focus here only on the structural peculiarities that are important for the lithium mobility in this material [11,14,15].

The iridium atoms in $LiIrSn_4$ have square-antiprismatic tin coordination. The antiprisms are condensed via common faces building the two-dimensional $[IrSn_4]$ polyanionic networks. The latter are connected via the lithium atoms. They have a square-prismatic tin coordination at Li–Sn distances of 291 pm. Such stuffed $LiSn_{8/8}$ cubes are the typical lithium coordination also in binary lithium stannides [25]. ^{7}Li solid-state NMR spectra [14] revealed a Knight shift of 9.2 ppm with respect to a 1 M LiCl aqueous solution. One can thus assume a significant charge transfer from lithium to the $[IrSn_4]$ network leading to an ionic formula splitting $Li^{\delta+}[IrSn_4]^{\delta-}$.

The chemical analyses of $LiIrSn_4$ via ICP-AES in our previous study [15] revealed a composition 1.06(2) Li: 1.08(2) Ir: 4.00(4)Sn, indicating full occupancy of the lithium sites. These results are in excellent agreement with the neutron diffraction study, while single crystal X-ray data did not allow for a refinement of the lithium occupancy parameter [15].

4.2. Electrochemical behaviour of $LiIrSn_4$

The coulometric titration curves (both deintercalation and intercalation) for $LiIrSn_4$ at 25 °C are shown in Figs. 3 and 4. For the as prepared sample, the initial open circuit voltage (OCV) of the cell was found to be 2.415 V. The OCVs of 6 samples prepared by the same synthetic route were very similar with 2.40($\pm$0.02) V. Titration current density was 0.25 mA/cm^2. As Fig. 3 shows, we started the electrochemical cycling in the deintercalation direction. During deintercalation of nearly $\Delta\delta \sim -0.02$, one already reaches a plateau, i.e. a nearly constant cell voltage of 2.75 V corresponding to a constant chemical potential of lithium. We assume that this discontinuity at $\Delta\delta \sim -0.02$ indicates that the lower limit of the lithium concentration is reached and that the ternary compound decomposes into at least two phases at the interface to the electrolyte. Any

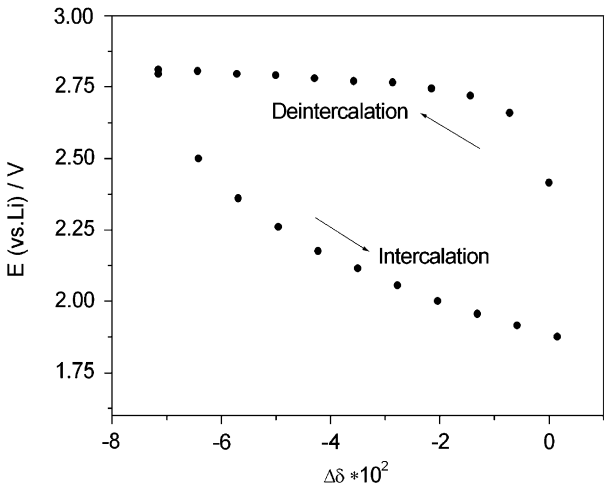

Fig. 3. Coulometric titration curve for polycrystalline $Li_{1+\Delta\delta}IrSn_4$ during deintercalation and intercalation at 25 °C.

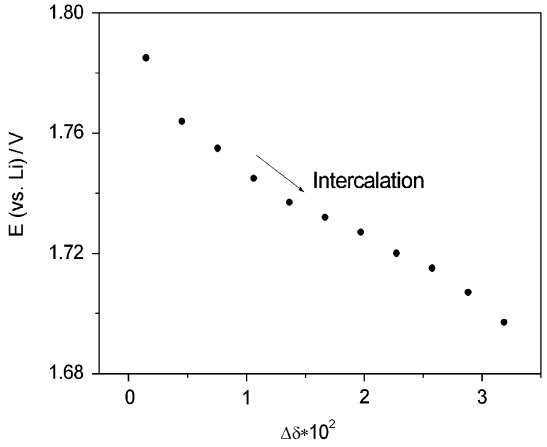

Fig. 4. Coulometric titration curve for polycrystalline $Li_{1+\Delta\delta}IrSn_4$ during intercalation at 25 °C.

further lithium extraction increases the amount of the new phases whereas the coexisting $LiIrSn_4$ takes a constant limiting stoichiometric composition. For a two phase equilibrium in a ternary system the phase rule predicts still one degree of freedom. If decomposition yields two additional phases, no degree of freedom would remain which explains our observation of a voltage plateau.

The coexisting second phase along with $LiIrSn_4$ is not completely understood. Although the phase diagram of the ternary system Li–Ir–Sn is not fully established we could predict the second phase appearing. The binaries IrSn [26], $IrSn_2$ [27], Ir_3Sn_7 [27], Ir_5Sn_7 [28], α-$IrSn_4$ [29,30] and its high pressure, high temperature modification β-$IrSn_4$ [31] have been reported so far in the literature. But one deduces any extraction of lithium from a phase with minimum lithium content must give at least two new phases to pertain the overall stoichiometric ratio Ir/Sn = 4. Therefore, in our case the most probable outcome of the lithium extraction would be

$$LiIrSn_4 \rightarrow Li + \alpha - IrSn_4.$$

At this point one should keep in mind that the iridium atoms in α-$IrSn_4$ have a distorted eightfold tin coordination. However, the whole crystal structure is trigonal in contrast to tetragonal $LiIrSn_4$. In order to understand the details of phase formation, further studies with in situ XRD measurements are required. Ex situ X-ray diffraction is not of much help since one complete cycle of deintercalation and intercalation results in the compound $Li_{1.012}IrSn_4$ which has a Guinier powder pattern matching that of the starting compound.

For each of the six samples which were prepared independently but with the same approach and the same composition of starting materials, we have got nearly the same result, i.e. the de-lithiation limit occurred at $\Delta\delta \sim -0.02$. This confirms that no considerable lithium deficiency can be observed for as prepared $LiIrSn_4$ which is also confirmed by neutron diffraction studies which narrow the lithium occupancy to 100(8)%.

In the second part of the coulometric experiments, we changed the direction of titration steps to injection of lithium. As can be seen in Fig. 3, the coulometric intercalation curve does not follow the path of the de-intercalation. The cell voltage decreases already remarkably during the first titration step and for all following steps. This behaviour is typical for a homogeneous one phase system. It is evident, that the α-$IrSn_4$ phase formed at the electrode/electrolyte interface resulting from the decomposition during de-intercalation cannot react back with electrochemically formed lithium to give $LiIrSn_4$ again. α-$IrSn_4$ has a trigonal crystal structure with the space group $P3_121$ [30]. As a result the intercalation of lithium into this phase would accompany a relatively huge lattice strain. So this different structure for α-$IrSn_4$ phase explains why we could not intercalate lithium back into this phase. This electrochemical observation supports the view of α-$IrSn_4$ being the inactive phase formed at the electrode/electrolyte interface. In addition, the missing ionic mobility in the lithium free decomposition products may be a reason for the irreversibility. Such an observation does occur at low temperatures. It is for instance also found for lithium intercalation with Li_xMnO_2 [32]. Therefore, the lithium intercalation in Fig. 3 does only concern the remaining ternary $LiIrSn_4$ (which is still present in excess). The measured cell voltage after each intercalation step (lower curve in Fig. 3) then corresponds to the true equilibrium chemical potential of lithium as a function of the changing non-stoichiometry.

Fig. 4 shows the continuation of intercalation from Fig. 3. It has been enlarged so that one can clearly see an inflection point at $\Delta\delta = 0.0133$ and $E = 1.74$ V. An inflection point within a coulometric titration curve usually occurs at the ideal stoichiometric composition of a solid. Therefore, the inflection point should correspond to the ideal stoichiometric composition, $LiIrSn_4$. But, in compounds with a small stoichiometric existence range, the ideal stoichiometric point usually shows the largest slope of the coulometric titration curve which means that there is a minimum of defect concentration. Our ternary compound shows the opposite behaviour, i.e. a minimum slope at the inflection point. This is found in typical intercalation compounds, if half of the available sites in a structure are filled by the intercalating component. In that case, neglecting interaction between the intercalating ions, Fermi–Dirac statistics yields the following formula for the chemical potential of lithium where x_{Li} denotes the fraction of (equivalent, iso-energetical) sites occupied by lithium [33]

$$FE = \mu_{Li} - \mu^0_{Li}/(RT) = \ln[x_{Li}/1 - x_{Li}]. \quad (5)$$

The diffusion coefficients were determined from the relaxation experiments for which the cell voltage changed, i.e. for the cell voltages below 2.75 V.

The interpretation curve resulting from Figs. 3 and 4 is shown in Fig. 5. This gives a much clearer picture of the stoichiometric existence range of the compound. The

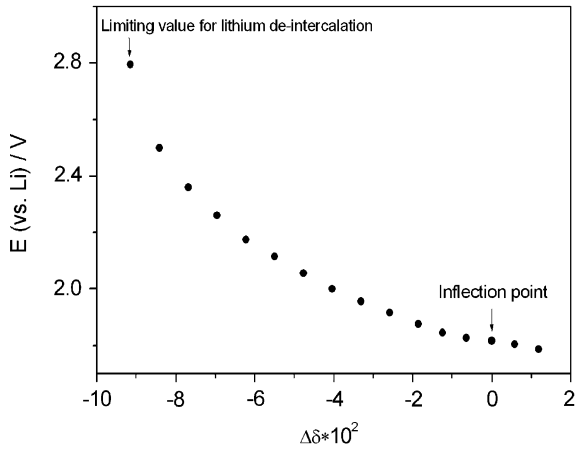

Fig. 5. Interpretation curve plotted with inflection point assigned to the stoichiometric $LiIrSn_4$ and showing the limiting lithium composition reached during deintercalation.

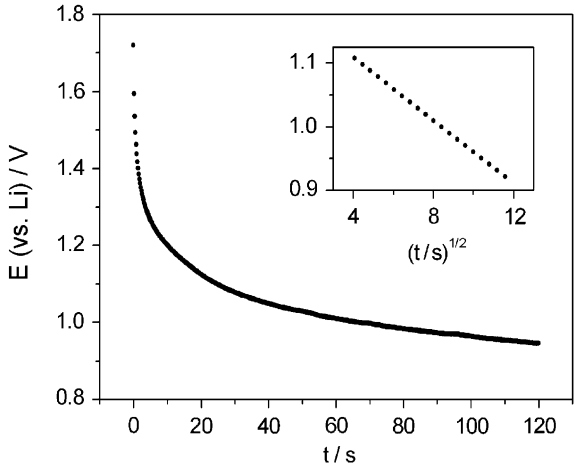

Fig. 6. Typical voltage response during a polarisation experiment with the employed working cell at 25 °C. Inset shows the verification of Cottrell equation using short time approximation.

inflection point which is observed in Fig. 4 at $\Delta\delta = 0.0133$ has been assigned to zero in Fig. 5. Also the intercalation curve, in Fig. 3, has been shifted so that now intercalation starts from the delithiation point ($\Delta\delta \sim -0.02$) which is marked in Fig. 5 as limiting value for lithium de-intercalation. From this the existence range of the ternary stannide, $Li_{1+\Delta\delta}IrSn_4$, $-0.091 \leqslant \delta \leqslant +0.012$ could be easily figured out. Note that we did not observe a limiting value for increasing lithium concentration. But the large change of the chemical potential (corresponding to a change of the cell voltage of nearly 1 V) within this small range of $\Delta\delta$ shows that $LiIrSn_4$ does not have a large stoichiometric existence range which is desired for an intercalation electrode such as the classical Li_xTiS_2 with $0 < x < 1$ [6,34].

Fig. 6 gives a typical voltage response of the working cell during a galvanostatic step with respect to time. The polarisation current was 0.56 mA. Cottrell's equation (Eq. (3)) was verified by checking the linear behaviour of the E vs. $t^{1/2}$ plot at sufficiently short times and consequently the chemical diffusion coefficient D_{Li} was determined.

Fig. 7 shows a corresponding result for potentiostatic steps. Measurements were done within a potential range 2.5 and 2.9 V vs. Li reference. Eq. (4) was verified as seen in the semi logarithmic plot in the inset.

From galvanostatic and potentiostatic measurements, the chemical diffusion coefficients were calculated using Eqs. (3) and (4). The values as obtained are found to be almost the same for both chronopotentiometric and chronoamperometric measurements. The D_{Li} value calculated using chronopotentiometry falls in the range 2×10^{-7}–8×10^{-9} cm^2/s. For chronoamperometry the value falls in the range 1×10^{-7}–9×10^{-8} cm^2/s. Similar values of diffusion coefficients were reported, for instance, for the binaries $Li_\delta Sn$ [21].

The D_{Li} value determined chronopotentiometrically is plotted as a function of the nonstoichiometry parameter $\Delta\delta$ in Fig. 8. During intercalation of the compound.

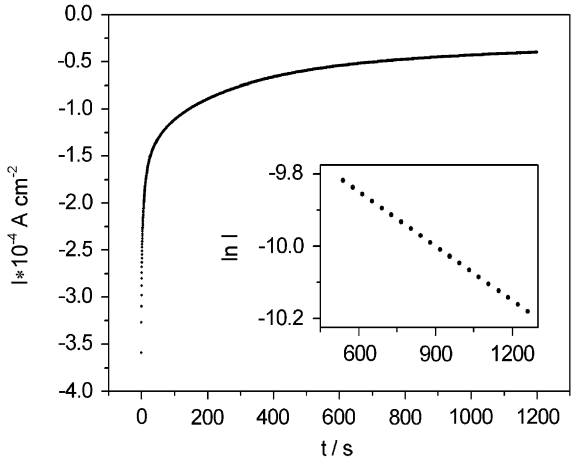

Fig. 7. Current vs. t plot using potentiostatic conditions and in the inset the linearity of the Cottrell equation is verified at 25 °C.

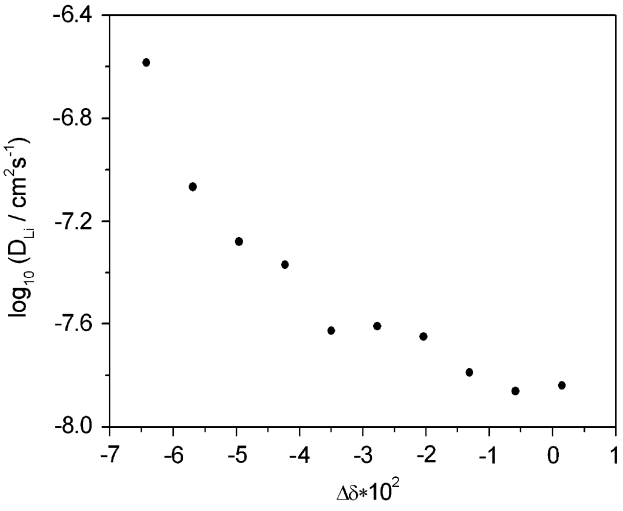

Fig. 8. Dependence of the chemical diffusion coefficient, D_{Li} on composition for $LiIrSn_4$ at 25 °C.

$Li_{1-\Delta\delta}IrSn_4$ the value of D_{Li} is found to decrease and then becomes a constant in the range around the ideal stoichiometry, i.e. around the experimental value $\Delta\delta = 0.0133$. This behaviour of the chemical diffusion coefficient is in accordance with the measured titration curve, the slope of which is proportional to the thermodynamic factor (or enhancement factor) which figures in the determination of the chemical diffusion coefficient. Therefore, we assume that the dependence of the chemical diffusion coefficient on the non-stoichiometry is mainly due to that of the thermodynamic factor [33].

The cyclic voltammogram for our electrochemical cell was also measured. The scan range of the voltage was 0–3 V with a scan rate of 1 mV/s. The first few cycles, the cathodic currents decrease. This is due to the non-reversibility of the deintercalation/intercalation step, because every cycle leaves some amount of decomposition products on the surface. No clear cathodic or anodic peaks were observed which is explainable by the slow lithium diffusion that limits the oxidation/reduction rate.

5. Conclusions

Ternary lithium alloys Li_xTX_z represent a broad class of novel materials. As this contribution showed, lithium electrode properties can be expected from them. The studies on $LiIrSn_4$ as the first electrochemically investigated example did not show optimum electrode properties in a sense that a broad range of lithium non-stoichiometries could be obtained. But with regard to our experience on the structure and available lithium sites in many other representatives of this class of compounds, we expect to find better candidates with higher reversibility of lithium intercalation as well as with a larger width of the non-stoichiometry. With regard to the chemical potential of lithium, there is a trend towards low values. This must be due to the noble metal content. Therefore, some of these intercalation materials may be candidates as cathode materials. So similar neutron diffraction and electrochemical studies is a viable tool on route to characterise ternary lithium alloys as electrode materials for lithium ion batteries.

Acknowldgments

We are indebted to the Degussa-Hüls AG for a generous gift of iridium powder. This work was financially supported by the Deutsche Forschungsgemeinschaft through SFB 458: *Ionenbewegung in Materialien mit ungeordneten Strukturen—vom Elementarschritt zum makroskopischen Transport*). P.S. is indebted to the NRW Graduate School of Chemistry for a Ph.D. stipend.

References

[1] J.O. Besenhard, Handbook of Battery Materials, Wiley-VCH, Weinheim, 1999.
[2] C.J. Wen, C. Ho, B.A. Boukamp, I.D. Raistrick, W. Weppner, R.A. Huggins, Int. Metals Rev. 5 (1981) 283.
[3] J.O. Besenhard, J. Yang, M. Winter, J. Power Sources 68 (1997) 87.
[4] J.O. Besenhard, P. Komenda, A. Paxinos, E. Wudy, M. Josowicz, Solid State Ionics 18&19 (1986) 823.
[5] J. Wang, I.D. Raistrick, R.A. Huggins, J. Electrochem. Soc. 133 (1986) 457.
[6] M. Winter, J.O. Besenhard, M.E. Spahr, P. Novak, Adv. Mater. 10 (1998) 725.
[7] K.D. Kepler, J.T. Vaughey, M.M. Thackeray, Electrochem. Solid-State Lett. 2 (1999) 307.
[8] W. Weppner, W. Sitte, Z. Naturforsch. A: Phys. Sci. 42 (1987) 1.
[9] J.R. Dahn, I.A. Courtney, J. Electrochem. Soc. 144 (1997) 2045.
[10] I.A. Courtney, J.S. Tse, O. Mao, J. Hafner, J.R. Dahn, Phys. Rev. B: Condens. Matter 58 (1998) 15583.
[11] R. Pöttgen, Zh. Wu, R.-D. Hoffmann, G. Kotzyba, H. Trill, J. Senker, D. Johrendt, B.D. Mosel, H. Eckert, Heteroatom Chem. 13 (2002) 506.
[12] Zh. Wu, B.D. Mosel, H. Eckert, R.-D. Hoffmann, R. Pöttgen, Chem. Eur. J. 10 (2004) 1558.
[13] Zh. Wu, H. Eckert, B.D. Mosel, R. Pöttgen, Z. Naturforsch. B: Chem. Sci. 58 (2003) 501.
[14] Zh. Wu, H. Eckert, J. Senker, D. Johrendt, G. Kotzyba, B.D. Mosel, H. Trill, R.-D. Hoffmann, R. Pöttgen, J. Phys. Chem. B 107 (2003) 1943.
[15] Zh. Wu, R.-D. Hoffmann, R. Pöttgen, Z. Anorg. Allg. Chem. 628 (2002) 1484.
[16] Zh. Wu, R.-D. Hoffmann, D. Johrendt, B.D. Mosel, H. Eckert, R. Pöttgen, J. Mater. Chem. 13 (2003) 2561.
[17] H.-S. Kim, P. Periasamy, S.-I. Moon, J. Kor. Electrochem. Soc. 7 (2004) 1.
[18] R.A. Huggins, C.J. Wen, J. Solid State Chem. 35 (1980) 376.
[19] R.A. Huggins, W. Weppner, J. Electrochem. Soc. 124 (1977) 1569.
[20] D. Rahner, S. Machill, J. Power Sources 54 (1995) 428.
[21] W. Weppner, W. Sitte, Appl. Phys. A 38 (1985) 31.
[22] R. Pöttgen, Th. Gulden, A. Simon, GIT Labor-Fachzeitschrift 43 (1999) 133.
[23] K. Yvon, W. Jeitschko, E. Parthé, J. Appl. Crystallogr. 10 (1977) 73.
[24] T. Roisnel, J. Rodríguez-Carvajal, FULLPROF 2k V. 2.0, 2001, 91191 Gif-sur-Yvette Cedex, France.
[25] W. Müller, U. Frank, Z. Naturforsch. B: Chem. Sci. 30 (1975) 316.
[26] H.W. Mayer, M. Ellner, K. Schubert, J. Less-Common Met. 61 (1978) 1.
[27] O. Nial, Sven. Kem. Tidskr. 59 (1947) 172.
[28] B. Künnen, D. Niepmann, W. Jeitschko, J. Alloys Compd. 309 (2000) 1.
[29] K. Lazar, P. Bussiere, Hyp. Int. 41 (1988) 559.
[30] A. Lang, W. Jeitschko, J. Mater. Chem. 6 (1996) 1889.
[31] S.V. Popova, V.I. Larchev, J. Less-Common Met. 98 (1984) L1.
[32] S. Jouanneau, S. Sarciaux, A. Le Gal La Salle, D. Guyomard, Solid State Ionics 140 (2001) 223.
[33] J. Maier, Physical Chemistry of Ionic Materials, Wiley, New York, 2004.
[34] M.S. Whittingham, Prog. Solid State Chem. 12 (1978) 41.